

DAN-AERO MW: Comparisons of airfoil characteristics for two airfoils tested in three different wind tunnels

Christian Bak
Helge Aa Madsen
Mac Gaunaa
Uwe Paulsen

Peter Fuglsang

Jonas Romblad
Niels A. Olesen

Peder Enevoldsen
Jesper Laursen

Leo Jensen

*Risø DTU National
Laboratory for
Sustainable Energy,
4000 Roskilde,
Denmark*
chba@risoe.dtu.dk

*LM Wind Power
Jupitervej 6
6000 Kolding
Denmark*
pfu@lmglasfiber.com

*Vestas Wind Systems
Alsvej 21,
8900 Randers
Denmark*
jorom@vestas.com

*Siemens Wind Power
Borupvej 16
7330 Brande
Denmark*
pe@siemens.com

*DONG Energy,
Kraftværksvej 53,
Skærbæk,
7000 Fredericia
Denmark*
leoje@dongenergy.dk

Abstract

This paper describes wind tunnel measurements carried out within the collaborative, three year DAN-AERO MW research project between Risø DTU and the industrial partners LM Wind Power, Siemens Wind Power, Vestas Wind Systems and the utility company DONG Energy from 2007 to 2009. One of the issues in the project was to explore the differences between airfoil characteristics measured in different wind tunnels. When designing a rotor and predicting the overall wind turbine performance using e.g. aeroelastic codes, the airfoil characteristics are crucial. Thus, in this work measurements on the NACA 63₃-418 and the Risø-B1-18 airfoils carried out in the VELUX wind tunnel (DK), the LM Wind Power Low Speed Wind Tunnel (DK) and the Delft Low Speed Low Turbulence wind tunnel (NL) were compared. The tunnels are different with respect to configuration and turbulence level.

The comparisons between the measurements showed that the best agreement between results was seen for Reynolds number of 3.0×10^6 because the LM and Delft tunnels were designed to work optimally around this Reynolds number.

Turbulence intensity of ~1% caused high drag coefficients at all angles of attack compared to turbulence intensities from 0.1% and below. Furthermore, turbulence intensities from 0.1% and below did not correlate with minimum drag. However,

the turbulence intensity had an influence on the transition point location. Thus, the lower the turbulence intensity, the higher the lift value at which the transition point moves towards the leading edge.

Several deviations between the wind tunnel data were observed, but most of the differences between the measurements were ascribed to differences in airfoil model shapes, methods for analyzing the data and calibrations.

A comparison of the measurements to XFOIL revealed the necessity to be aware of the turbulence intensity. It also revealed the limitations in XFOIL, where the drag coefficient in general was under predicted and maximum lift as well as the lift under separated conditions was significantly over predicted.

Keywords: Airfoils, airfoil characteristics, wind tunnel

1 Introduction

Designing wind turbine rotors require detailed knowledge of aerodynamic and structural airfoil characteristics. The aerodynamic airfoil characteristics are commonly revealed either by two-dimensional computations or by measurements in wind tunnels. Even though the computational methods have matured to the point where they can be used with high confidence, wind tunnel measurements are very important because some parameters such as maximum lift, stall characteristics and the

level of drag seems to deviate somewhat from computations.

Furthermore, the derivation of 3D airfoil characteristics from 2D wind tunnel characteristics still introduces uncertainty and conservatism in the rotor design process although different empirical correction methods have been developed [1,2,3,4,5].

However, even though correction is needed also more confidence of airfoil characteristics from wind tunnels is needed. Thus, in the process of designing a rotor and an entire wind turbine, entities such as maximum lift, lift-drag ratio, zero-lift-angle-of-attack and the slope of the lift curve are important.

Several types of wind tunnels exist, which roughly can be distinguished by the following elements:

- Return/open circuit wind tunnels, where the air is either recirculated or new air is entering the tunnel all the time, respectively.
- Open/closed test sections, where the flow in the test section either is confined or is entering the test sections as a jet, respectively.
- Boundary layer e.g. flow quality and turbulence level

Furthermore, parameters such as the contraction ratio, which is the ratio between the area of the cross sections at the low speed part of the tunnel and the area of the high speed part just upstream of the test section, diffuser angle downstream of the test section, aspect ratio of the cross section in the test section and the chord-to-test-section-height are important. Because of the interaction between the lift and drag forces and the flow, all airfoil measurements in wind tunnels need correction. The correction is more significant in open test sections than in closed test sections.

In this work comparisons are carried out between the commonly used NACA 63₃-418 airfoil [6] and the wind turbine dedicated high lift airfoil Risø-B1-18 [7] measured in the three different wind tunnels:

- The VELUX wind tunnel (DK)
- The LM Wind Power Low Speed Wind Tunnel (LSWT) (DK)

- The Delft Low Speed Low Turbulence (LSLT) tunnel (NL)

For the NACA 63₃-418 airfoil additionally available data from the Stuttgart LWK (GER) and the Langley LTPT (USA) were shown in the comparison of the data.

Key values for the different wind tunnel layouts are related to the test results.

2 Experimental setup and approach

Two different airfoil designs were tested: The commonly used NACA 63₃-418 airfoil designed for airplanes and the wind turbine dedicated high lift airfoil Risø-B1-18. One NACA 63₃-418 airfoil model and one Risø-B1-18 airfoil model with chord length 0.600m were used in both the VELUX tunnel and the Delft tunnel. For the LM Wind Power tunnel new models were manufactured with a chord length of 0.900m.

Tests were carried out at $Re=1.5 \times 10^6$ and 1.6×10^6 . For the Delft and LM tunnel $Re=3 \times 10^6$ was also tested. Different configurations were tested such as clean surface and leading edge roughness in terms of zigzag tape at the leading edge.

2.1 The airfoils

NACA 63₃-418

The NACA 63₃-418 airfoil is described by Abbott and Doenhoff [6] and is designed for use on airplanes. However, it has been extensively used in the wind turbine industry for a few decades, because of the relatively smooth stall characteristics, the relatively high insensitivity of maximum lift to leading edge roughness, the quite good aerodynamic performance and the good structural characteristics. The intended use for airplanes causes the maximum lift-drag ratio to appear at a rather low lift coefficient ($c_l \sim 0.9$) and with a medium maximum lift coefficient ($c_{l,max} \sim 1.3$ for Reynolds numbers between 1.5 and 3×10^6).

Risø-B1-18

The Risø-B1-18 airfoil is described by Fuglsang and Bak [7] and is designed for wind turbines and specifically for those with Pitch Regulation and Variable rotor Speed (PRVS). For this type of regulation, stall is to a great extent avoided and the stall characteristics require less consideration. The airfoil is designed to be

insensitive of maximum lift to leading edge roughness, to have high maximum lift ($C_{l,max} \sim 1.6$) and to show maximum lift-drag ratio at a quite high lift coefficient ($C_l \sim 1.3$ for Reynolds numbers between 1.5 and 3×10^6). The two airfoil contours are shown in Figure 1.

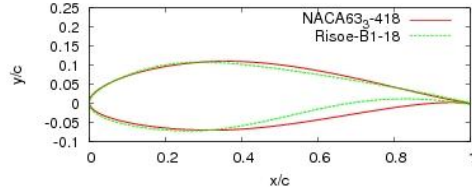


Figure 1: The NACA 63₃-418 and the Risø-B1-18 airfoil contours.

2.2 The leading edge roughness

With the requirement of 20 years wind turbine operation it is unavoidable that the blades surface condition will vary especially at the leading edge. The surface will change either because of contamination caused by dust and bugs sticking to the surface or by erosion. Thus, apart from testing airfoils with a clean surface, also leading edge roughness (LER) should be simulated in wind tunnel tests. However, there is still no consensus of how to do it. In this work four different types of roughness were used:

1. Zigzag tape mounted at $x/c=0.05$ at the suction side and at $x/c=0.10$ at the pressure side with a tape thickness of 0.4mm, a tape width of 3mm and a tape pattern of 90°.
2. Zigzag tape mounted at $x/c=0.02$ at the suction side with a tape thickness of 0.4mm, a tape width of 3mm and a tape pattern of 90°.
3. Zigzag tape mounted at $x/c=0.05$ at the suction side and at $x/c=0.10$ at the pressure side with a tape thickness of 0.4mm, a tape width of 3mm and a tape pattern of 60°.
4. Sandpaper 3M Safety-Walk of width 0.15m (6inch) wrapped around the leading edge covering the entire airfoil from the leading edge to $x/c=0.08$ on both pressure and suction side.

Only the first type of simulation was used in all the tunnels, whereas the second was used only in the LM LSWT and the third and fourth were used in the Delft tunnel. In this paper only the results from the first roughness simulation type will be compared. With a constant thickness of the zigzag tape in all the tunnels, the relative thickness in the LM tunnel was

$t/c=4.4 \times 10^{-4}$ and 50% higher in the LM and Delft tunnels, $t/c=6.7 \times 10^{-4}$

2.3 The tunnels

Below the three wind tunnels are described. However, also the Stuttgart LWK and the NASA Langley LTPT are described because measured characteristics for the NACA 63₃-418 airfoil from these tunnels are also shown here. In all wind tunnels the drag was measured using a wake rake (an arrangement of parallel total pressure tubes in the wake of the airfoil). Thus, the pressure distribution (or the pressure/velocity deficit) in the wake of the airfoil is measured and converted to a drag coefficient.

VELUX wind tunnel

This wind tunnel is situated in Østbirk, Denmark, is owned by the roof top window manufacturer VELUX and is of the closed return type. The test section is open and the turbulence intensity is relatively high, $Tl=1\%$. The airfoil forces are measured using pressure taps in the airfoil surface and the drag is measured using a fixed wake rake. The distributed pressure measurements are integrated to lift, drag and moment coefficients. The forces are corrected with respect to down wash and stream line curvature, see Ref. [8]. The test stand is mobile and owned by Risø DTU, so the measurements are carried out in campaigns over three to four days. The tunnel has been used by Risø DTU since the start of the 1990'ies. The dimensions of the tunnel are seen in Table 1.

LM Wind Power LSWT

This wind tunnel is situated in Lunderskov, Denmark, is owned by LM Wind Power and is of the closed return type. The test section is closed and the turbulence intensity is relatively low, $Tl=0.1\%$. The airfoil forces are measured using airfoil surface pressure taps and the drag is measured using a traversing wake rake. The distributed pressure measurements are integrated to lift, drag and moment coefficients and corrected according to Fuglsang and Bove [9]. The tunnel has been active since 2006. The dimensions of the tunnel are seen in Table 1.

The Delft LSLT

This Low Speed Low Turbulence (LSLT) wind tunnel is situated in Delft, The Netherlands, at Delft University of Technology. It is of the closed return type

and the test section is closed. The turbulence intensity is very low, $TI=0.02\%$. The airfoil forces are measured using the same principles as in the LM tunnel and lift, drag and moment coefficients are integrated and corrected according to the method described by Timmer [10]. The dimensions of the tunnel are seen in Table 1.

The Stuttgart LWK

This Stuttgart Laminar Windkanal (LWK) was not part of the general comparisons, but was used because one of the two airfoils was measured in the tunnel. It is situated in Stuttgart, Germany, at Stuttgart University and is of the open type and the test section is closed. The turbulence intensity is extremely low, $TI=0.0002\%$. The airfoil forces are measured using pressure taps on the wind tunnel walls and the drag is measured using a traversing wake rake. The distributed pressure measurements are integrated to lift and drag coefficients and corrected, see Althaus [11]. The dimensions of the tunnel are seen in Table 1.

The NASA Langley LTPT

As for the Stuttgart wind tunnel, this tunnel was not part of the general comparisons, but was used because one of the airfoils was measured at one Reynolds number. It is situated in Hampton, Virginia, USA, at the NASA Langley Research Center and is a Low Turbulence Pressure Tunnel (LTPT). It is of the closed return type and the test section is closed. The turbulence intensity is unknown, but is probably similar to the turbulence level in the Delft tunnel, because of the similarities in contraction ratio. The airfoil forces are measured using pressure taps on the wind tunnel walls and the drag is measured using a wake rake. The dimensions of the tunnel are seen in Table 1. A further feature of this tunnel is the possibility of increasing the pressure from 1 atm to 10 atm increasing the density and thereby increasing the Reynolds number. The tunnel has been used for test of a huge number of e.g. NACA airfoils, which are reported by e.g. Abbott and Doenhoff [6].

Summary of the wind tunnels

In Table 1 a summary of the tunnels is seen in terms of key parameters. The knowledge of these parameters is important for interpretation of the results, because the boundary and initial conditions for the tunnel flow affect the airfoil performance. The question is how the following parameters influence the performance:

- The turbulence intensity: A high turbulence intensity will move the transition from laminar to turbulent flow towards the leading edge. However, energy spectra of the turbulence are unspecified.
- The wind tunnel blockage: The ratio between the height of the test section and the chord length is a measure of how the walls/jet boundary will interact with the airfoil forces.
- The aspect ratio: The ratio between the chord length and the span width of the airfoil model gives an indication of the degree of two-dimensionality of the flow.
- Fixed or traversing wake rake: The wake rake can either be fixed to measure the velocity deficit in one plane or the wake rake can be traversed to integrate possible changes along the airfoil span.

The above list of parameters is not ment to be complete, but shows some of the very important factors that can contribute to deviations in measurements between wind tunnels.

Finally, from the limited list of wind tunnels, Table 1, there is a relation between contraction ratio, cr , and turbulence intensity, TI , that follows the function: $cr[-] = 4(TI[\%])^{0.38}$. However, according to the theory, Barlow *et al.* [12], the relation should for the longitudinal direction be $cr[-] \sim TI(U)[\%]^{0.5}$ and for the lateral direction $cr[-] \sim TI(V)[\%]^2$, which do not agree with the observation. As stated by Barlow *et al.*, there does not appear to be a good method of predicting the effects of contraction ratios in turbulence reduction. Thus, to support the validity of the above observed relation significantly more wind tunnels have to be analyzed.

Table 1: Key parameters describing the dimensions and setup of the wind tunnels.

Tunnel	Return	Test section	Test section length, L [m]	Test section/jet height, H [m]	Test section width, W [m]	Ti [%]	Chord length, c [m]	Height-chord ratio H/c [-]	Aspect ratio, W/c [-]	Contraction ratio	Maximum speed [m/s]	Lift measurement	Wake rake
VELUX	Closed	Open	7.50	3.40	1.90	1.0	0.60	5.7	3.2	3.11	40	Airfoil	Fix
LM	Closed	Closed	7.00	2.70	1.35	0.1	0.90	3.0	1.5	10	105	Airfoil	Trav
Delft	Closed	Closed	2.60	1.80	1.25	0.02	0.60	3.0	2.1	17.8	120	Airfoil	Trav
Stuttgart	Open	Closed	3.15	2.73	0.73	0.0002	0.60	4.55	1.2	100	90	Wall	Trav
Langley	Closed	Closed	2.29	2.29	0.91	-	0.60	3.81	1.5	17.6	130	Wall	-

3 Results

The airfoils were tested in the three tunnels at $Re=1.6 \times 10^6$ in Delft [13] and VELUX [14] and at $Re=1.5 \times 10^6$ in LM [15,16]. Also, the airfoils were tested at $Re=3.0 \times 10^6$ in Delft and at LM, but not in the VELUX wind tunnel. Furthermore, the NACA 63₃-418 airfoil was tested at $Re=1.5 \times 10^6$ and 3×10^6 in the Stuttgart LWK and at $Re=3 \times 10^6$ in the Langley LTPT. Key parameters extracted from the wind tunnel measurements are seen for $Re=1.5/1.6 \times 10^6$ and 3.0×10^6 for the NACA 63₃-418 airfoil in Table 2 and for the Risø-B1-18 airfoil in Table 3.

The measurements at $Re=3 \times 10^6$ in clean configurations are compared to XFOIL, Drela [17]. XFOIL is a panel code with inviscid/viscous interaction and for a given angle of attack, AoA , and Re , it provides the c_p -distribution and lift and drag coefficients. Transition from laminar to turbulent flow was modeled by the e^n method with $n = 9$ corresponding to $Ti=0.07\%$. Investigations carried out by Bertagnolio *et al.* [18] showed that XFOIL for thin airfoils in many cases over predicts and delayed maximum lift slightly compared to EllipSys2D [19,20,21]. Later, Bertagnolio *et al.* [22] investigated 3D airfoil computations using different turbulence models, which showed significant differences in the prediction of maximum lift. However, at low angles of attack both XFOIL and EllipSys predicted the airfoil performance quite well.

3.1 NACA 63₃-418

Reynolds number 1.5×10^6

Figure 2 shows results for the clean configuration. Here, also data from the Stuttgart tunnel is included for comparison. It is seen that there is no exact agreement between the data from the different tunnels. There are several deviations between the measurements.

The determination of the zero-lift-angle-of-attack, AoA_0 , from the different tunnels is measured within the range of 1.3 degrees. This can be due to uncertainties in measuring the geometric AoA , shape deviations in the airfoil contour and corrections of the measured lift.

The slopes of the linear part of the lift curve agree fairly well between 0.111 and 0.116 per degree (between $2\pi+0.077\text{rad}^{-1}$ and $2\pi+0.363\text{rad}^{-1}$) with a somewhat higher slope in the Delft tunnel and lower slope in the VELUX tunnel. The slope seems not to correlate with the wind tunnel layout parameters shown in Table 1.

The maximum lift coefficients, $c_{l,max}$, agree fairly well between 1.23 and 1.33. It is noted that the AoA , at which $c_{l,max}$ appears, $AoA_{c_{l,max}}$, increases with increasing ratio of H/c . This means that a reduction in blockage could be the reason for an increase in $c_{l,max}$. However, several other parameters determine the level of $c_{l,max}$ such as Ti [23], the aspect ratio and whether the lift measurement is carried out on the tunnel walls or on airfoil surface. Also, the quality of the models determines the level. However, to the extent that these parameters are known they do not correlate with the variations in $c_{l,max}$.

Table 2: Key values describing the aerodynamic performance of the NACA 63₃-418 in clean surface configuration

	$Re \times 10^6$	AoA_0	$C_{l,max}$	$AoA_{cl,max}$	$C_{d,min}$	$Max(C_l/C_d)$	$AoA_{Max(cl/cd)}$	$C_{l,Max(cl/cd)}$
Delft	1.6	-2.5	1.23	11.3	0.0064	119.5	6.1	1.00
LM	1.5	-3.5	1.31	11.1	0.0083	101.1	5.1	0.94
Stuttgart	1.5	-3.3	1.32	12.3	0.0072	110.9	5.7	1.02
VELUX	1.6	-2.2	1.33	16.3	0.0093	73.0	5.0	0.80
Delft	3.0	-2.5	1.30	12.8	0.0062	121.1	5.2	0.91
LM	3.0	-3.2	1.35	11.7	0.0054	134.8	5.1	0.93
Stuttgart	3.0	-3.0	1.30	10.9	0.0062	114.7	4.4	0.86
Langley	3.0	-2.8	1.38	13.3	0.0060	121.6	6.1	1.01

Table 3: Key values describing the aerodynamic performance of the Risø-B1-18 in clean surface configuration

	$Re \times 10^6$	AoA_0	$C_{l,max}$	$AoA_{cl,max}$	$C_{d,min}$	$Max(C_l/C_d)$	$AoA_{Max(cl/cd)}$	$C_{l,Max(cl/cd)}$
Delft	1.6	-3.6	1.55	11.8	0.0080	122.6	8.2	1.36
LM	1.5	-4.3	1.50	11.4	0.0074	125.3	7.1	1.21
VELUX	1.6	-3.3	1.64	13.5	0.0090	100.2	6.5	1.16
Delft	3.0	-3.5	1.68	12.3	0.0072	135.8	7.2	1.30
LM	3.0	-3.9	1.66	12.9	0.0067	129.7	6.1	1.15

The drag coefficient, c_d , differs somewhat and especially in the VELUX tunnel which has a rather high TI compared to the other tunnels. Because the Delft tunnel shows the lowest minimum drag values, $C_{d,min}$, there seems however not to be a clear correlation between TI and $C_{d,min}$, since the Stuttgart tunnel has lower TI than the Delft tunnel. However, parameters such as the degree of two-dimensionality of the flow and the method of measuring the wake deficit can also affect the prediction of c_d . Somewhat fluctuating c_d from the LM tunnel seems to appear, which probably is caused by less sensitivity of the measurement equipment, because it is calibrated for Reynolds numbers between $Re=3 \times 10^6$ and 6×10^6 .

Figure 3 shows data for the LER configuration (zigzag tape mounted on suction side at $x/c=0.05$ from the leading edge and on pressure side at $x/c=0.10$ from the leading edge). Here, only data from Delft and VELUX is available with the prescribed zigzag tape. Also, measurements from Stuttgart [11] are shown with a somewhat different way of simulating the leading edge roughness. The data from Delft and VELUX agrees very well, however with somewhat higher c_d in the VELUX tunnel. The data from Stuttgart is not based on the same LER simulation and cannot be directly compared. However, it shows the same trends in the decrease in $C_{l,max}$ and increase in c_d .

Reynolds number 3.0×10^6

Figure 4 shows results for the clean configuration. Here, the VELUX tunnel is not part of the comparisons, because this

Reynolds number is above the range of this tunnel. However, data from the Stuttgart and the Langley tunnels are included for comparison.

It is seen that the agreement between the data in the different tunnels are much better than at $Re=1.6 \times 10^6$ for the clean configuration. However, there are still some deviations between the measurements.

The determination of AoA_0 from the different tunnels is measured within the range of 0.7 degree. As for the lower Reynolds number this can be due to uncertainties in measuring the geometric AoA , shape deviations in the airfoil contour and corrections of the measured lift.

The slopes of the linear part of the lift curve agree fairly well between 0.112 and 0.120 per degree (between $2\pi+0.114\text{rad}^{-1}$ and $2\pi+0.592\text{rad}^{-1}$) with a somewhat higher slope in the Delft tunnel and lower slope in the Langley tunnel. As was the case for the lower Reynolds number, the slope seems not to correlate with the wind tunnel layout parameters shown in Table 1.

Agreement of $C_{l,max}$ is fairly good between 1.30 and 1.38. No correlations between the $AoA_{cl,max}$ and the four parameters 1) the ratio H/c , 2) TI , 3) the ratio W/c and 4) whether the pressure is measured on the airfoil surface or on the walls have been detected as was the case at the lower Reynolds number.

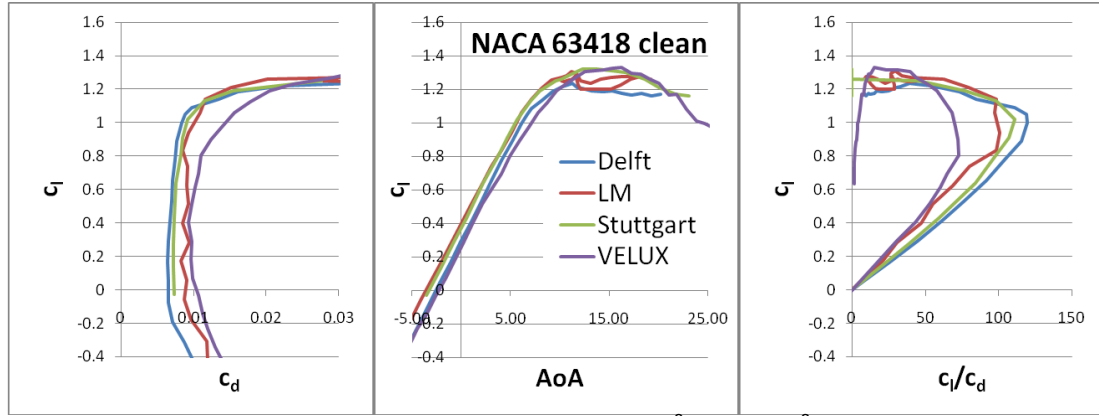


Figure 2: Polars for NACA63₃-418 airfoil at $Re=1.5 \times 10^6$ to 1.6×10^6 in clean configuration.

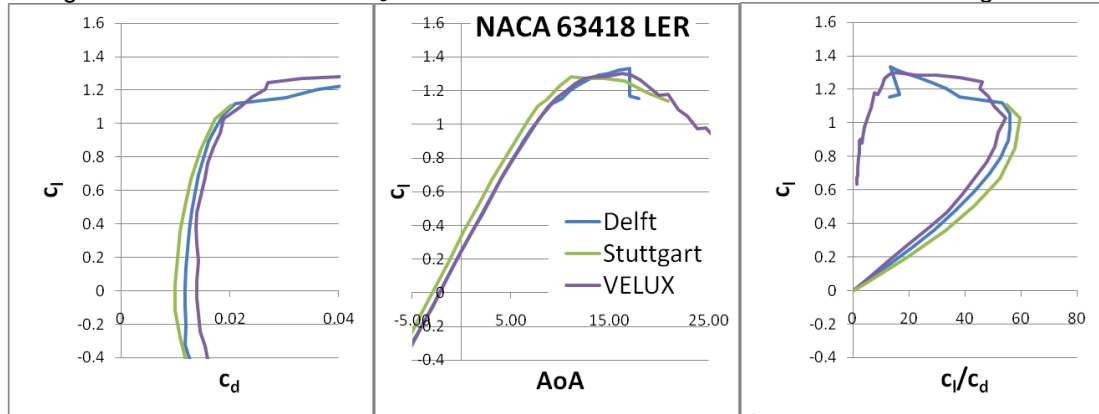


Figure 3: Polars for NACA63₃-418 airfoil at $Re=1.6 \times 10^6$ in LER configuration.

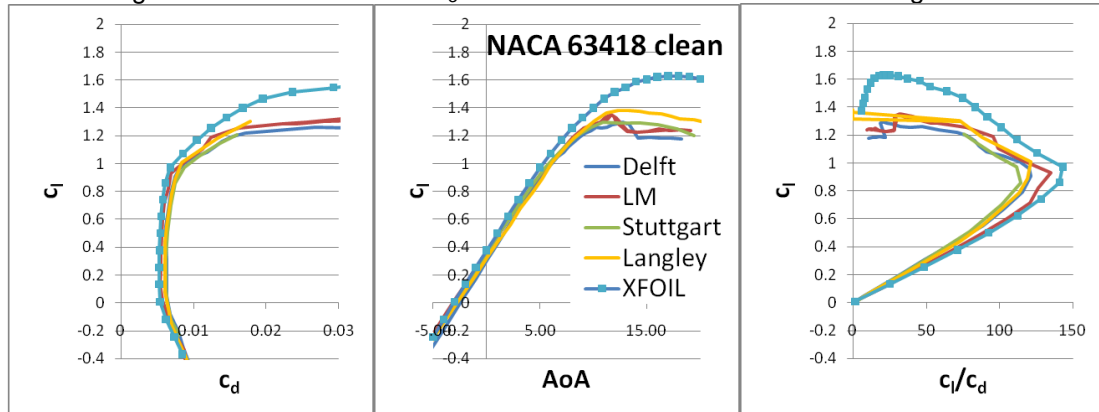


Figure 4: Polars for NACA63₃-418 airfoil at $Re=3.0 \times 10^6$ in clean configuration.

Agreements of c_d are quite well at all lift coefficients with $c_{d,min}$ between 0.0055 in the LM tunnel and 0.0062 in the Stuttgart tunnel. Because the LM tunnel with the highest Tl (which is quite low) shows the lowest c_d and the Stuttgart tunnel with lowest Tl shows the highest c_d , an expected reduction in c_d with a reduction in Tl is not observed.

Since c_d depend on more parameters than Tl such as the airfoil surface quality, the resolution of the pressure tubes in the wake rake measuring the pressure in the airfoil wake, the method used to detect the wake and the Mach number, no

conclusions regarding correlation of the drag measurements to the wind tunnel configuration can be drawn.

Finally, the results with clean configuration are compared to XFOIL computations. It is seen that XFOIL predicts the aerodynamic performance well at low AoA, however with somewhat under predictions of c_d . At high AoA XFOIL seems to over predict $c_{l,max}$ and c_l for separated flows significantly.

3.2 Risø-B1-18

Reynolds number 1.5×10^6

The Risø-B1-18 airfoil was like the NACA 63₃-418 airfoil tested in the three tunnels at $Re=1.6 \times 10^6$ at Delft and VELUX and at $Re=1.5 \times 10^6$ at LM. Figure 5 shows data for the clean configuration and Figure 6 shows data for the LER configuration at $Re=1.5/1.6 \times 10^6$.

As for the NACA 63₃-418 airfoil at $Re=1.6 \times 10^6$ it is seen that there is no exact agreement between the data in the different tunnels for the clean configuration. The results deviated from each other in several ways.

The determination of AOA_0 from the different tunnels is within 1.0 degree. As for the NACA 63₃-418 airfoil this can be due to uncertainties in measuring the geometric AoA, shape deviations in the airfoil contour and corrections of the measured lift.

The slopes of the linear part of the lift curve differ somewhat between 0.106 and 0.122 per degree (between $2\pi-0.21\text{rad}^{-1}$ and $2\pi+0.71\text{rad}^{-1}$), again with somewhat higher slope in the Delft tunnel and lower slope in the LM tunnel. However, the slope seems not to correlate with the wind tunnel layout parameters shown in Table 1.

Significant differences are seen for $c_{l,max}$ and the stall characteristics, between 1.48 and 1.64. Since the VELUX tunnel shows the highest $c_{l,max}$ there might be a correlation between on one hand the ratio H/c , the ratio W/c or whether the test section is open or closed and on the other hand $c_{l,max}$. However, other parameters such as TI might influence the measurements significantly. Thus, there is no clear correlation between $c_{l,max}$ and the wind tunnel layout.

Some differences are seen for c_d and especially in the VELUX tunnel as was the case for the NACA 63₃-418 airfoil. Thus, the measurements show that high TI affects c_d , but that TI below a certain level does not affect the determination of $c_{d,min}$. However, comparing the c_l vs c_d plot, Figure 5, a “knee” in the curve is seen for both LM and Delft data. The knees appear at $c_l \sim 1.3$ for the LM data and at $c_l \sim 1.4$ for the Delft data. The knees indicate the lift levels at which the transition from laminar to turbulent flow moves towards the leading edge. Thus, it seems that the somewhat higher TI or the given energy

spectra of the turbulence in the LM tunnel affects the transition from laminar to turbulent flow in an earlier stage than the Delft tunnel.

For the LER configuration c_l from Delft and VELUX agrees very well, however with somewhat higher c_d in the VELUX tunnel and more abrupt stall in the Delft tunnel.

Reynolds number 3.0×10^6

The Risø-B1-18 airfoil was tested in only two tunnels, Delft and LM, at $Re=3.0 \times 10^6$. Figure 7 shows results for the clean configuration and Figure 8 shows data for the LER configuration at $Re=3.0 \times 10^6$.

It is seen that there is very good agreement between the data in the two tunnels for the clean configuration. However, the results deviated from each other in a few ways.

The determination of AoA_0 from the different tunnels is within 0.4 degree. No other reasons for this than those mentioned for the test at the lower Reynolds number are known.

The slopes of the linear part of the lift curve differ somewhat between 0.115 and 0.123 per degree (between $2\pi+0.31\text{rad}^{-1}$ and $2\pi+0.76\text{rad}^{-1}$), again with somewhat higher slope in the Delft tunnel and lower slope in the LM tunnel.

Very similar values of $c_{l,max}$ is seen, between 1.66 and 1.68, and also the stall characteristics are very similar.

Also, the c_d values are very similar. However, as was the case at $Re=1.6 \times 10^6$, the knee of the c_l vs c_d plot appears at different c_l for the two tunnels. In the Delft tunnel the knee appears at higher c_l , indicating lower TI , which is in good agreement with the specifications for the tunnels. Thus, as long as TI is fairly low ($\leq 0.1\%$) it seems that it does not affect c_d very much. However, it seems to affect the dynamics of the transition point location.

For the LER configuration c_l from Delft and LM agrees very well, but with some difference in $c_{l,max}$, between 1.62 and 1.72.

The determination of AoA_0 is within 0.5 degrees in this case. Also, differences are seen in c_d , with higher c_d in the Delft tunnel. Thus, some deviations in aerodynamic performance are observed for the Risø-B1-18 airfoil when comparing the clean configuration with the LER configuration.

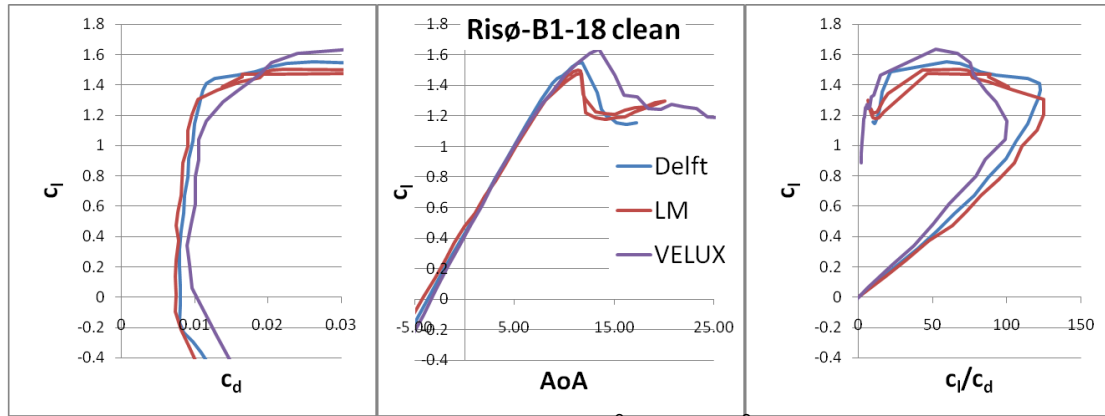


Figure 5: Polars for Risø-B1-18 airfoil at $Re=1.5 \times 10^6$ to 1.6×10^6 in clean configuration.

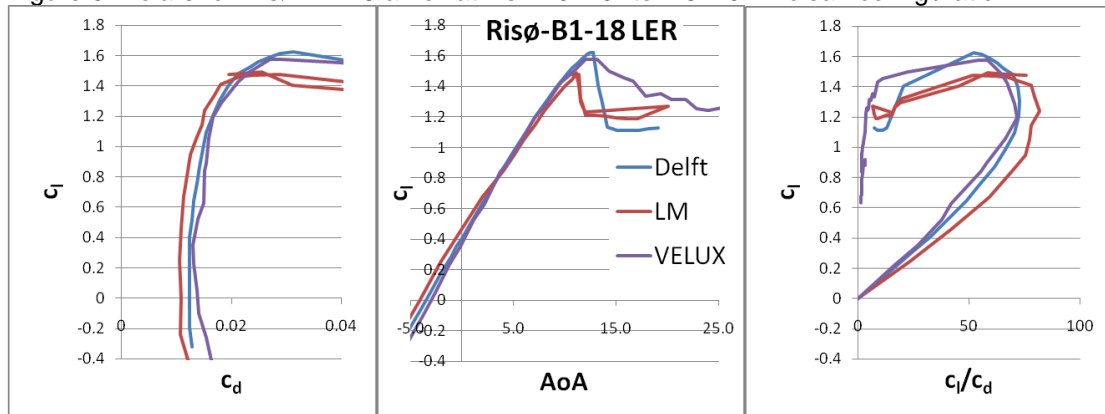


Figure 6: Polars for Risø-B1-18 airfoil at $Re=1.5 \times 10^6$ to 1.6×10^6 in LER configuration.

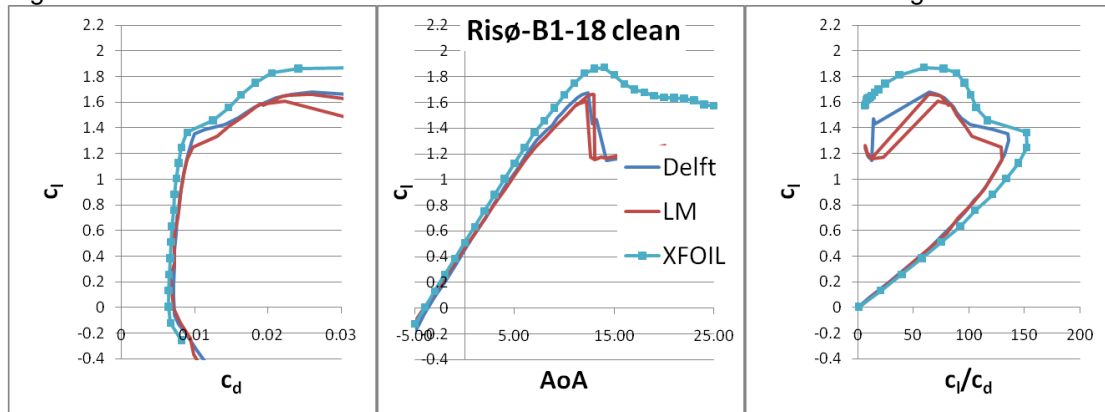


Figure 7: Polars for Risø-B1-18 airfoil at $Re=3.0 \times 10^6$ in clean configuration.

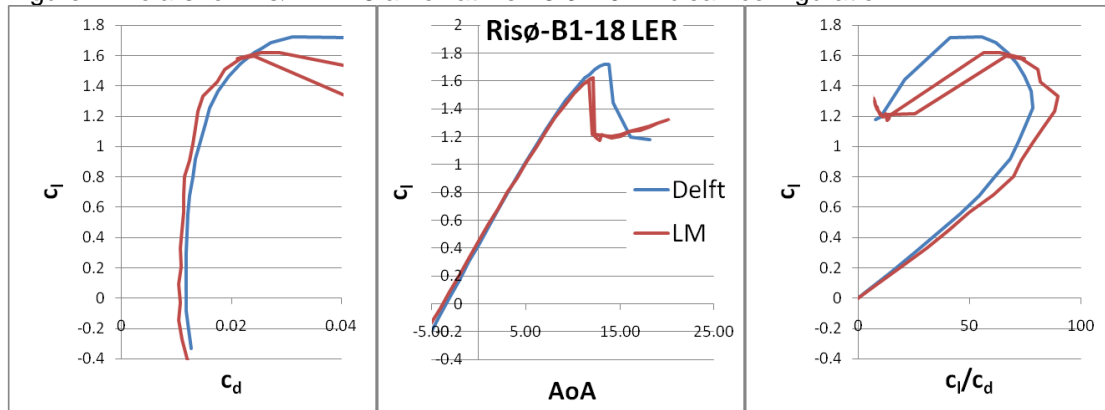


Figure 8: Polars for Risø-B1-18 airfoil at $Re=3.0 \times 10^6$ in LER configuration.

This can however be due to small differences in the geometry of the zigzag tape and the relatively thicker zigzag tape as stated in section 2.2, or the way the zigzag tape was mounted on the airfoil surface.

Finally, the data with clean configuration is compared to XFOIL computations using the e to the n^{th} method with $n=9$. It is seen that XFOIL predicts the aerodynamic performance well at low AoA, however with somewhat under predictions of c_d . Especially the knee at the c_l vs c_d plot is quite well predicted. At high AoA, the measurements do not agree very well with the predictions and XFOIL over predicts $c_{l,max}$ and c_l for the separating airfoil significantly.

4 Conclusions

This paper showed polars measured in the LM Wind Power LSWT, the Delft LSLT tunnel and the VELUX tunnel carried out in the DAN-AERO MW project. Comparing the polars revealed differences in zero-lift-angle-of-attack, the slope of the linear part of the lift curve, maximum lift, the stall characteristics and the drag. Here, also a few measurements carried out in the Stuttgart LWK and the Langley LTPT were used for the comparisons. Even though the wind tunnel tests deviated in several ways, only the general conclusions will be emphasized here.

The best agreement between results was seen for Reynolds number of 3.0×10^6 . The results for Reynolds numbers of 1.6×10^6 deviated somewhat from each other. This was probably due to the (lack of) sensitivity of the measurement equipment and the calibration of the wind tunnels, because the tunnels are designed to work at different Reynolds numbers.

With the rather high turbulence intensity of 1% in the VELUX tunnel all comparisons of polars showed significantly higher drag values in the VELUX tunnel. However, for the rest of the wind tunnels it seems that the minimum drag was not influenced by the turbulence intensity. Thus, with a turbulence intensity below a certain value, which is minimum TI=0.1%, minimum drag seems to be unaffected by the turbulence level. However, the transition point location seems to be affected by the turbulence intensity, so that differences in the airfoil performance will be seen clearly,

if fast changes appear in the transition point location.

No clear correlation between on one side the maximum lift, the stall, the zero-lift angle-of-attack and the slope of the linear part of the lift curve and on the other side the wind tunnel layout could be identified. However, this might be due to counteracting mechanisms such as extremely low turbulence intensity, which could tend to reduce maximum lift, combined with a relatively high ratio between test section height and chord length, which might increase the maximum lift.

Thus, most of the differences between the measurements are ascribed to differences in airfoil model shapes, methods for analyzing the data and calibrations.

In addition, the measurements were compared to XFOIL computations. This comparison revealed the necessity to be aware of e.g. the turbulence intensity when using airfoil characteristics for wind turbine design. It also revealed the limitations in XFOIL, where the drag coefficient in general was under predicted and maximum lift and the lift on the separating airfoil was significantly over predicted. Furthermore, the comparisons between measurements and the predictions by XFOIL stress the necessity to carry out wind tunnel measurements to validate the flow simulations.

When validating the airfoil performance in a wind tunnel, this work revealed the importance of specifying the turbulence intensity. It is however not known for the time being, which turbulence intensity that represents atmospheric flow on wind turbine blades. This is under investigation in the DANAERO MW II project using transition measurements on a 2.3MW rotor compared with transition characteristics in the LM LSWT. The DANAERO MW II project is carried out in the period 2010 to 2011 in collaboration between Risø DTU, LM Wind Power, Vestas Wind Systems and Siemens Wind Power.

5 Acknowledgements

This project was funded partly by the Danish Energy Authorities, EFP2007, and partly by eigenfunding from the project partners. Also, this project was only possible because of skilled people at the different partners.

References

- [1] Snel, H.; Houwink, R.; van Bussel, G.J.W.; Bruining, A., 'Sectional Prediction of 3D Effects for Stalled Flow on Rotating Blades and Comparison with Measurements', Proc. European Community Wind Energy Conference, Lübeck-Travemünde, Germany, 8-12 March, 1993, pp. 395-399, H.S. Stephens & Associates
- [2] Du, Z.; Selig, M.S., 'A 3-D Stall-Delay Model for Horizontal Axis Wind Turbine Performance Prediction', AIAA-98-0021, 36th AIAA Aerospace Sciences Meeting and Exhibit, 1998 ASME Wind Energy Symposium, Reno, NV, USA, January 12-15, 1998
- [3] Chaviaropoulos, P.K.; Hansen, M.O.L., 'Investigating Three-Dimensional and Rotational Effects on Wind Turbine Blades by Means of a Quasi-3D Navier Stokes Solver', J. Fluids Engineering, vol. 122, June 2000, pp. 330-336.
- [4] Lindenburg, C., "Modelling of Rotational Augmentation Based on Engineering Considerations and Measurements", European Wind Energy Conference, London, 22-25 November 2004
- [5] Bak, C.; Johansen, J.; Andersen, P.B.; Three-Dimensional Corrections of Airfoil Characteristics Based on Pressure Distributions; Presented at the European Wind Energy Conference & Exhibition (EWEC), 27. Feb. – 2. Mar. 2006, Athens, Greece
- [6] Abbot, I.H.; von Doenhoff, A.E.; Theory of wing sections: including a summary of airfoil data; New York, Dover publications Inc., 1959, 693 p.
- [7] Fuglsang, P.; Bak, C.; Development of the Risø wind turbine airfoils; Wind Energy, Volume 7 Issue 2, Pages 145-162
- [8] Fuglsang, P.; Antoniou, I.; Sørensen, N.N.; Madsen, H.A., 'Validation of a Wind Tunnel Testing Facility for Blade Surface Pressure Measurements, Risø-R-981(EN), Risø National Laboratory, Roskilde, April 1998
- [9] Fuglsang, P.; Bove, S.; Wind Tunnel Testing Of Airfoils Involves More Than Just Wall Corrections, European Wind Energy Conference 2008 (EWEC2008) Brussels, paper CW2.2, 1.-4. April 2008
- [10] Timmer, W.A.; WECS-blade airfoils-the NACA 63-4xx series. Proc. European Community Wind Energy. Conference Madrid, Spain, September 1990
- [11] Althaus, D., "Niedriggeschwindigkeitprofile", Vieweg Verlagsgesellschaft; Auflage: 1 (1996), ISBN-10: 3528038209, ISBN-13: 978-3528038205
- [12] Barlow, J.B.; Rae Jr., W.H.; Pope, A.; Low-Speed Wind Tunnel Testing, Third edition, John Wiley & Sons, Inc., 1999
- [13] Timmer, W., "Wind tunnel test results for airfoils NACA 633-418 and Risø B1-18", WE-082063, Delft University of Technology, Faculty of Aerospace Engineering, Wind Energy Research Group, May 2008
- [14] Fuglsang P, Bak C, Gaunaa M, Antoniou I. Wind tunnel Tests of Risø-B1-18 and Risø-B1-24. Risø-R-1375(EN), Risø National Laboratory, Denmark, January 2003.
- [15] Müller, O., "LSWT Report of Campaign NACA 63-418 1, Public Version", LM Glasfiber, Rev : 1.0, June 16, 2009
- [16] Müller, O., "LSWT report of Campaign Risø-B1-18", LM Glasfiber, Rev : 3.0, March 24, 2009,
- [17] Drela M. *XFOIL, An Analysis and Design system for Low Reynolds Number Airfoils. Low Reynolds Number Aerodynamics*, volume 54. In Springer-Verlag Lec. Notes in Eng., 1989.
- [18] Bertagnolio, F.; Sørensen, N.; Johansen, J.; Fuglsang, P., 'Wind Turbine Airfoil Catalogue', Risø-R-1280(EN), Risø National Laboratory, Roskilde, Denmark August 2001
- [19] Sørensen, N.N., 1995, 'General Purpose Flow Solver Applied to Flow over Hills', Risø-R 827(EN), Risø National Laboratory, Denmark
- [20] Michelsen, J.A., 'Basis3D – a Platform for Development of Multiblock PDE Solvers', Technical Report AFM 92-05, Technical University of Denmark, (1992)

[21] Michelsen, J.A., 'Block Structured Multigrid Solution of 2D and 3D Elliptic PDE's', Technical Report AFM 94-06, Technical University of Denmark, (1994)

[22] Bertagnolio, F.; Sørensen, N.N., Johansen, J., 'Profile Catalogue for Airfoil Sections Based on 3D Computations', Risø-R-1581(EN), Risø National Laboratory, Roskilde, Denmark, December 2006

[23] Bak, C.; Andersen, P.B.; Madsen, H.A.; Gaunaa, M.; Fuglsang, P.; Bove, S.; Design and Verification of Airfoils Resistant to Surface Contamination and Turbulence Intensity; AIAA 2008-7050, 26th AIAA Applied Aerodynamics Conference, 18 - 21 August 2008, Honolulu, Hawaii